SETTLEMENT OF WEAKLY CEMENTED TUFAS

NIHAT DIPOVA, M.UFUK ERGUN and VEDAT DOYURAN

about the authors

Nihat Dipova
Akdeniz University,
Department of Civil Engineering,
Antalya, Turkey
E-mail: ndipova@akdeniz.edu.tr

M. Ufuk Ergun
Middle East Technical University,
Department of Civil Engineering,
Ankara, Turkey
E-mail: eruf@metu.edu.tr

Vedat Doyuran
Middle East Technical University,
Department of Geol. Engineering,
Ankara, Turkey
E-mail: vedat@metu.edu.tr

Abstract

Weakly cemented tufas are sand and silt size soils that are weakly bonded with thin films of carbonate cement. The void ratio is rather high and equal to approximately 1.2. Collapse occurs as a result of the destruction of the weak bonds upon loading and/or wetting. The index properties and the collapse potential (C_p) of tufa were determined in the laboratory. In the determination of the collapse-potential values the single-ring oedometer method was considered to be a suitable and simpler tool. In plotting the oedometer test results the use of a natural scale was preferred over a logarithmic scale so that the void ratio-pressure relationship is polynomial. Under loading the soil settles with the natural water content; however, saturation increases the collapse that is initially triggered by the pressure increase. The pressure level is a significant parameter in the magnitude of the collapse and therefore in the total settlement. The settlement of foundations due to a collapse of the soil structure can be estimated directly using the oedometer test results and empirically using the index properties, like the initial void ratio (e_0), the difference in the fine content between the dry and the wet sieve analyses (PFAW) and the natural unit weight. A comparison of the direct and empirical approaches yielded a good agreement.

keywords

Antalya, collapse potential, collapsible soils, settlement, tufa

1 INTRODUCTION

Antalya, the study area, is a well-known tourist destination that is famous for its tufa coastal cliffs and wide beaches. These appealing features increased the population of Antalya and also the value of the land extending behind the cliffs, leading to high-rise constructions. However, some of these luxurious, high-rise buildings suffered from foundation instabilities. Cracking of the walls and a general tilting were typical indications of the foundation problems that the buildings suffered. The maximum tilting was observed on an 11-story building (Figure 1). The tilt amount was 1.6 degrees and the deflection at the top of the building was 85 cm. During construction the loading for every floor resulted in a

Figure 1. Leaning apartment building in Antalya (Turkey).

partial settlement at the natural water content of the soil. The pressure distribution under the foundation was non-uniform, which led to the differential settlement. To solve this, leveling concrete was applied. This resulted in an increased eccentricity and a large differential settlement. The water pipes broke due to the high shear force on the pipe. Leakage from the pipe through the foundation soil caused the saturation of the soil. After the saturation, maximum settlement occurs instantaneously. The foundation soils are composed of varieties of tufa, which can be classified as weakly cemented silt-sand [1]. The grains of the Antalya tufa deposits are bonded to each other by a meniscus cementation of thin calcium carbonate films. The cementation in these deposits is due to the deposition of calcium carbonate, carried downward by percolating water under unsaturated flow conditions. Later, rainwater or water leakage from pipes dissolves this thin film and destroys the interparticle bonding. As a consequence, the voids are closed and, finally, collapse occurs [2].

The geo-mechanical behavior of cemented materials is characterized by a high initial stiffness, which decreases after the yield due to the degradation of the bonding, and the progressive transformation of the cemented soil into a granular material [3]. Cemented sands, as well as the other structured soils, are considered as intermediate materials: they are stronger than soils but do not perform as rocks [4]. Cementation makes the soil stronger; however, the natural cementation tends to be highly irregular, causing significant spatial variations in strength over relatively short distances within a soil deposit, so making characterization difficult [5]. As a result of the cementation, carbonate sands exhibit true cohesion, which makes cemented sands stronger than uncemented sands. However, this apparent stiffness can suddenly be lost under loading when flooded. When soils show this behavior, they are called "collapsible soils".

Collapsible soils have a highly porous soil structure that sustains large stresses in the unsaturated state but collapses in a short time upon wetting, under constant total vertical stresses, leading to diverse consequences that affect the serviceability and stability of the structures supported by these soils. It is known that the collapsibility of soils depends on the soil porosity and moisture content [6, 7, 8]. A procedure was suggested in ASTM (2005) [9] to describe the collapse potential of a soil. According to this method, step loading is applied to the specimen up to a pressure level of 200 kN/m^2, using a conventional oedometer cell. At this pressure, the specimens are flooded. This test provides the natural void ratio (e_0), and the void ratios before (e_1) and after (e_2) the flooding. The collapse potential, C_p, can be calculated as:

$$C_p = \frac{e_1 - e_2}{1 + e}\ (100) \qquad (1)$$

where (e_1-e_2) represents the decrease in the void ratio on saturation and "e" is the initial void ratio of the soil specimen. Abelev (1948) [10] used "e" as the void ratio of the soil specimen before water was added at that particular pressure.

The mechanisms of collapse have been examined and reported for different types of soils, such as soft sensitive clays, loose unsaturated sands, silty sands and loess, residual soils and cemented alluvium [11, 12, 13, 14, 15, 16, 17]. The low interparticle bond strength, which is common for all cases, comes from clay bridges or weak meniscus cementation. Similar to other collapsible soils, collapsible tufas exhibit common properties. In collapsible tufas grains and cement are both calcium carbonate and the soil structure is more heterogeneous than for other types of collapsible soils.

The main purpose of this investigation is to clarify the settlement behavior of weakly cemented tufas upon loading and wetting. In this study, predictive models were developed to determine the collapse potential values through multiple regression analysis, stress-collapse-time relationships were investigated and finally analytical and empirical procedures have been developed for the prediction of the settlement of the foundations resting on collapsible tufas.

2 GEOLOGICAL BACKGROUND

The tufas are terrestrial carbonate units that precipitate by both physico-chemical and biogenic processes. The rate of precipitation affects the physical properties of the tufas. Lithoclast, intraclast and microdetrital tufas, which are deposited rapidly in the fluvial environments, form weakly cemented clastics and soft tufas. In contrast, in stagnant water in large-scale lacustrine environments, fine carbonates are deposited as hard micrite rock. The final appearance of the tufa is also dependent on post-depositional modifications (diagenesis). In the biogenic precipitation process, precipitation is the cause of the decreasing partial pressure of CO_2 by the photosynthesis of algae or bacteria. The daylight photosynthesis of blue-green algae results in the removal of CO_2 from the water in the day. Calcite crystals can be observed as hanging on the algae (Figure 2a). In very recent (<1 year) precipitates, on one fiber of algae, several crystals were hanging over, while in rather aged precipitates (e.g., at a depth of 2 m in a completely filled pool) the number of crystals increases, and in diagenetic rocks

a)

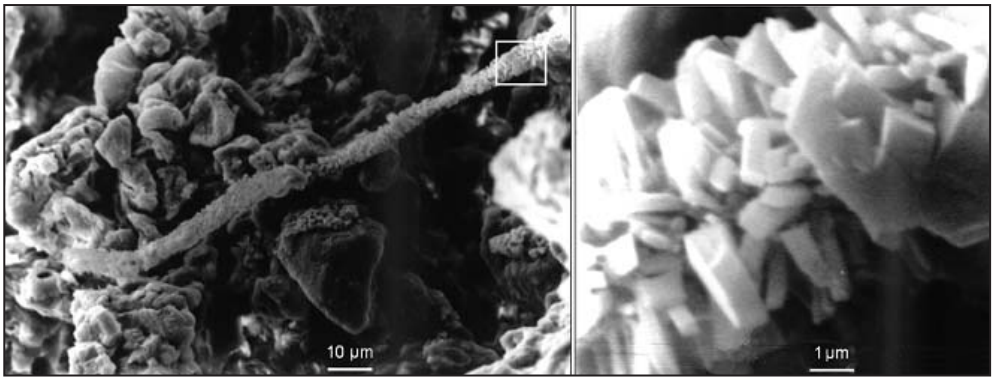

b)

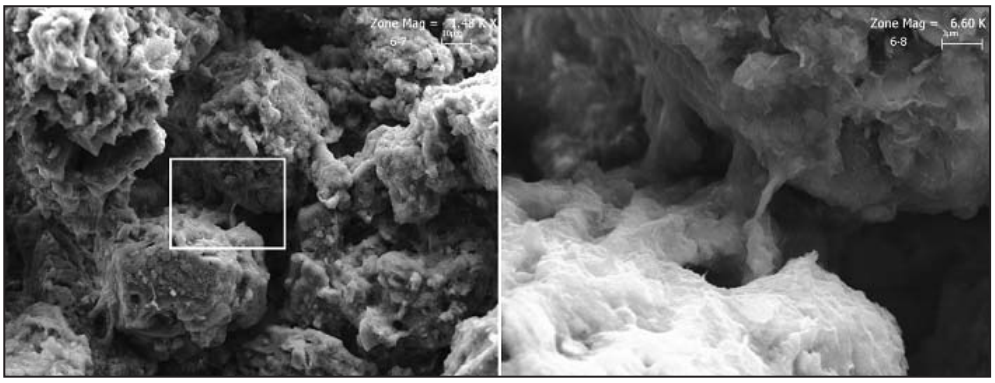

Figure 2. a) Scanning Electron Microscope (SEM) view of calcite cover around a fibrous algae (right), close up views of white rectangle (left), b) SEM view of meniscus cementation between tufa grains (left), close-up view (right).

spar micritization causes a completely covered calcite tube. After the precipitation or deposition of grains, diagenesis starts with meteoric cementation in the phreatic and vadose zones. Carbonate sediments in the vadose zone have often suffered less diagenetic modification. Recent sediments sampled from a depth of 4–6 m show only thin meniscus cements, concentrated at the grain contacts. However, this is only detectable in SEM analyses (Figure 2b). Where phreatic zone sediments or sediments through which water flows as seepage are available, spary-calcite cement development at the grain contacts and as void fill is possible.

Among tufa deposits, clastics (lithoclast, intraclast, phytoclast, oncoliths, pisoliths) and micro-clastics (micrite and peloidal tufa) may show soil-like behavior. These tufas are made of grain-supported sand and silt size grains. A weak meniscus cementation makes these deposits bonded, but with a highly porous soil structure. If these deposits do not contain secondary cavity fill cementation or re-crystallization, they can be classified as "weakly cemented soil" having the potential to be collapsible soils.

3 GEOTECHNICAL TESTING

For geotechnical testing purposes, 36 undisturbed soil samples were obtained from 2-m-deep test pits and excavation pits that were opened for various civil-engineering works. Due to the highly porous and brittle nature of the tufa, the preparation of laboratory specimens from the block samples was very difficult. To solve this problem, in this research, sampling from the walls of the excavation was preferred to the base. In this way the disturbance of the excavation machine is more effectively controlled and the soil type is properly observed. The pressure to push the sampler into the ground was applied hydraulically instead of manual pushing or hammering (Figure 3). High-quality, thin-walled, hard steel samplers with an area ratio of 8.5 % and a sharp cutting shoe were used. The inside of the sampler was covered with oil before the sampling. A series of laboratory tests was performed on the samples to determine the index and compressibility properties of weakly cemented tufas. Table 1 provides a summary of the test results.

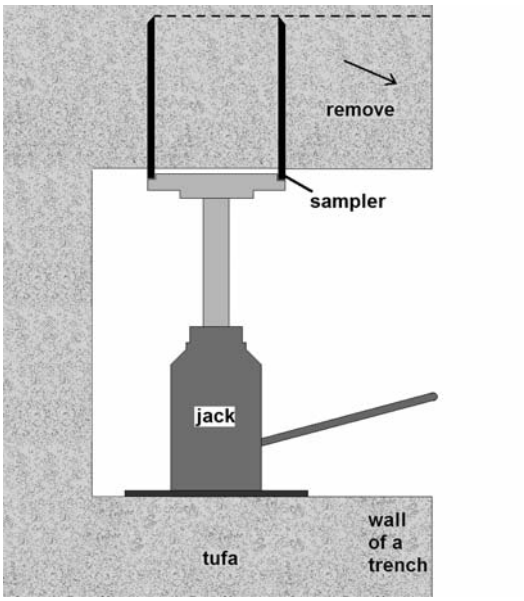

Figure 3. Method for field sampling of collapsible tufa from the wall of a trench.

Table 1. Mean and marginal values of the geotechnical properties.

Soil Property	Minimum	Mean	Maximum
Specific Gravity (G_s)	1.98	2.29	2.47
Dry Unit Weight (kN/m^3)	10.37	11.90	13.92
Initial Void Ratio (e_0)	0.703	1.254	1.666
Total Fines (D<63 mic) (%)	20	49.76	91
PFAW (%)	12	36	83
m_v (m^2/kN)	0.000054	0.000101	0.00018
C_p (%)	0.81	5.20	14.5

3.1 SPECIFIC GRAVITY, UNIT WEIGHT AND POROSITY

The specific gravity of the soils was determined according to ASTM D854-00e1 [18]. The maximum specific gravity value of five samples is G_s = 2.47, which is much less than the characteristic value for calcium carbonate minerals. This results from the determination technique and the material characteristics. The specific-gravity values were determined by applying a vacuum into the pycnometer. There must have been unreachable and closed micro-voids, and such voids can be seen on the SEM images. Taking into account the closed voids, for the void ratio calculations a theoretical value of G_s = 2.7 was used.

The unit weight of soils was determined for the oedometer test samples as the ratio of the soil weight to the internal volume of the ring. The void ratio of the soil specimens found in the oedometer tests ranged between 0.71 and 1.67, which classifies them as medium to highly porous in the IAEG classification system [19].

3.2 GRAIN SIZE DISTRIBUTION

The grains in the tufa samples are sand-silt-sized non-plastics. As the collapsible behavior is related to the weak cementation between the grains, the fine-material content gives an important clue regarding the degree of cementation of the grains. The performed grain size distribution tests were applied in accordance with the procedure suggested by ASTM D422-63 [20]. In dry conditions, due to the cementation between the grains, the dominant grain size is the sand size tufa lumps. In wet sieving, however, the cementation is destroyed and the fraction of the fines is increased (Figure 4). In wet sieving the soil is sieved by applying a tap-water flow through the 63-micron sieve without any dispersing agent. In this way only weak bonds, which dissolve in water without any frictional force or acidic agent, are disrupted. Saturation results in the dissolution of the carbonate bonds between the grains of lumps, and thus the solid grains become free, and finally the grain size decreases. A new parameter given in Dipova and Doyuran (2006b) [2] "Percent Fines After Wetting (PFAW)", which is in fact the difference in the fine fraction between the dry and wet sieving loosened after the dissolution of the soil lumps as a result of the saturation. This parameter is also used in the predictive models in this paper.

3.3 COMPRESSIBILITY AND COLLAPSIBILITY

To observe the compressibility and collapsibility of the soil specimens, standard oedometer tests were applied. Due to the highly porous and brittle nature of the tufa, special care was required during the preparation of the oedometer test samples from the 100-mm Shelby tube samples. A specially manufactured hydraulic sample extruder with two adapter plates was used (Figure 5). A little wetting of the soil around the ring was helpful when pushing the ring without any break up of the sample edge. A constant specimen diameter of 75 mm and a height of H = 20 mm were used. All the specimens were allowed to air-dry before testing.

Due to the sample heterogeneity and the difficulties encountered in the preparation of two samples that have

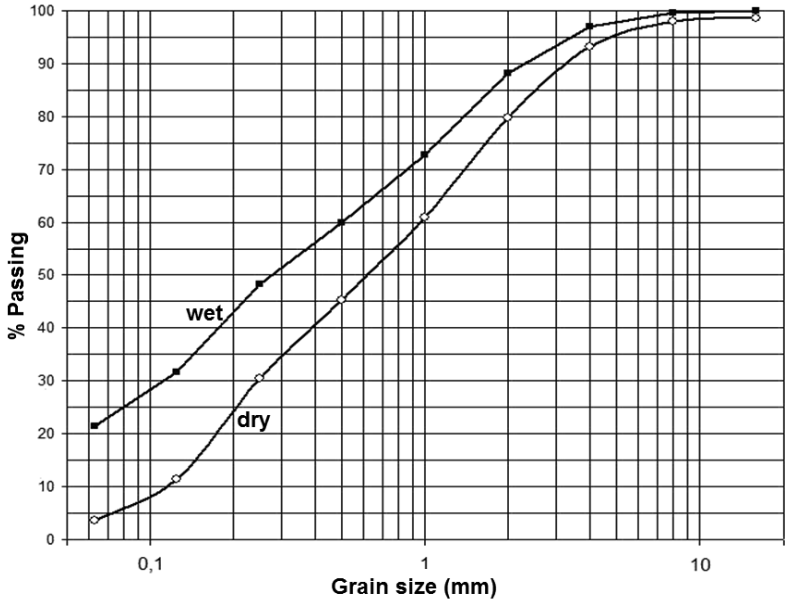

Figure 4. Grain size distribution after dry and wet sieving.

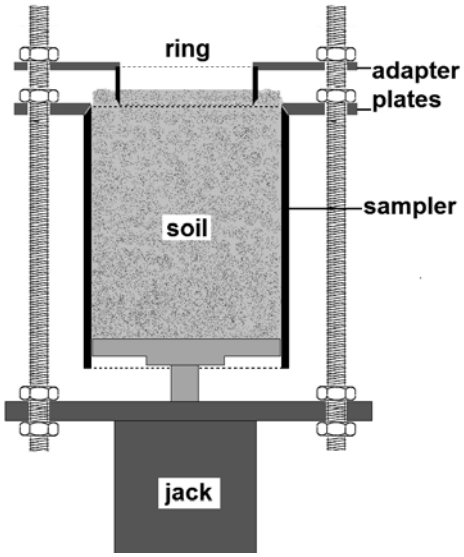

Figure 5. Sample extruder having two adapters set, which were used in the oedometer sample preparation.

the same initial void ratio for a double oedometer test, the tests were carried out by applying the "single-ring method" on a single specimen. The double-ring oedometer method is suitable for observing the differences in the deformation characteristics between the partially and fully saturated specimens at different stress levels. However, if the purpose of the test is to obtain a measure of the amount of volume change that occurs when a partially saturated soil becomes submerged under constant stress, it would be more practical and simpler to use the single-ring oedometer test.

In the oedometer test, a freshly undisturbed unsaturated specimen is incrementally loaded (the load increment ratio is unity) to a desired vertical stress (200 kPa in this study) without wetting the specimen. The samples were saturated at a stress of 200 kPa and the collapse potentials were determined at this stress level. The time-settlement readings during unsaturated loading, during the collapse process and after the collapse, were continuously recorded with the aid of sensitive electronic deformation sensors and an analog-to-digital converter (ADC) interface. By step loading before and after the 200 kPa, the behavior of the soil under dry (at the natural water content) and fully saturated conditions was determined. In particular for the prediction of the settlement under dry conditions before wetting, a determination of the volume compressibility (m_v) is possible in this way. The collapse potential of an unsaturated specimen was calculated from equation (1) taking "e" as the void ratio of the soil specimen before the water saturation.

4 GEOTECHNICAL EVALUATIONS

The mechanism for collapse includes an increase in the loading and/or an increase in the water content. In this section the collapse will be discussed for weakly cemented tufa for the air-dry condition (dry) and for the fully saturated state (wet). Similar to the investigated foundation settlement of buildings on weakly cemented tufa, a total collapse that results from loading and saturation should be considered.

4.1 STRESS LEVEL-COLLAPSE POTENTIAL RELATIONSHIP

To investigate the stress level-collapse potential relationship, a group of samples was tested in the laboratory and the collapse deformations were measured at different stress levels. To create a hydro-collapse, the samples were saturated at different stress levels, ranging between 25 kPa and 400 kPa. Typical compression curves are shown for dry and saturated samples in Figure 6. From this figure it is concluded that for both curves the trend is polynomial within the testing limits. The vertical distance between these two polynomial lines at any pressure level gives the void ratio difference (e_1-e_2) upon saturation. In the figure it is also clear that the void ratio difference (e_1-e_2) changes almost linearly up to 200 kPa. Thus, for small foundation pressures, the collapse potential changes almost linearly with pressure.

4.2 TIME-SETTLEMENT RELATIONSHIP

To assess the rate of settlement, the one-dimensional deformation during the oedometer tests was measured using an electronic deformation sensor and stored on a computer. The recorded data were plotted on time-settlement graphs (Figures 7 and 8). In both the dry and wet loading the rate of settlement is rather high. In the dry-loading phase, just after the load application, 80 % of the collapse settlement occurred in less than an hour. The remaining settlement occurred as a creep-like deformation throughout the day (Figure 7). For the same sample, after 24 hours in the dry condition, saturation results in a collapse, which causes a large displacement with respect to the dry loading (Figure 8). The rate of settlement was higher than that of the dry phase. Almost 95 % of the total settlement was completed in an hour, and 5 % of the deformation was creep. This behavior implies that the

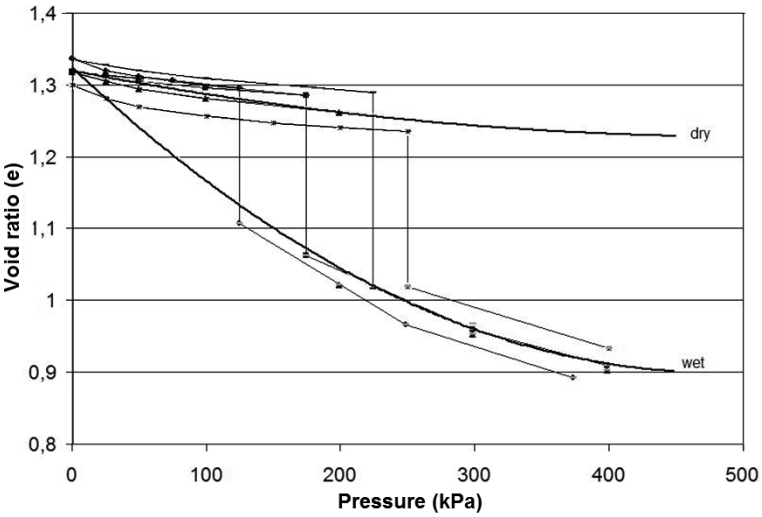

Figure 6. Stress level-collapse potential relationship of a group of tufa samples.

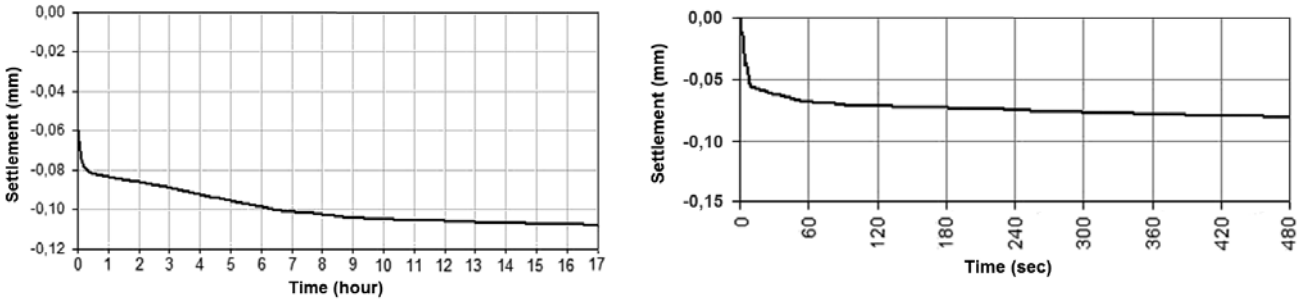

Figure 7. left - Time-settlement curve of tufa under 100 kPa pressure (dry),
right - Time-settlement curve of tufa under 100 kPa pressure (dry) (close up view).

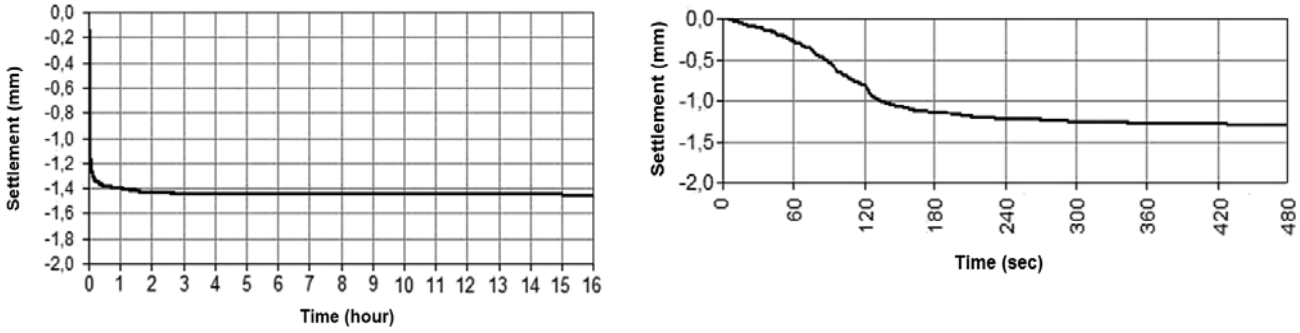

Figure 8. left - Time-settlement curve of tufa under 100 kPa pressure (wet), right - Time-settlement curve of tufa under 100 kPa pressure (wet) (close up view).

destruction of the inter-particle bonding occurs relatively quickly. The time for the completion of the settlement, even if it is relatively short, should have been spent for the re-arrangement of the particles and the stress re-distribution cycles, up to the final arrangement.

4.3 STATISTICAL EVALUATIONS AND PREDICTIVE MODELS

In the face of the complicated behavior of the collapsible tufa deposits and the various parameters that affect it, an alternative route would be the development of prediction models that can, to some extent, substitute expensive and time-consuming laboratory techniques. Although the laboratory techniques are quite reliable, for a quick appraisal of the collapse potential, an empirical method based on simple index tests for the prediction of foundation settlement will be helpful.

The values of the collapse potential (C_p) change over a wide range. However, statistical analyses showed that C_p is in a relatively close relationship with the initial void ratio (e_0) and the difference in the fine content between dry and wet sieving (PFAW) and also with the natural unit weight (γ_n). Similarly, another statistical analysis was performed to search for relationships between the coefficient of volume compressibility (m_v), e_0 and PFAW. Utilizing the results of multiple regression analyses the following best-fit equations were found to obtain the C_p and m_v parameters (Equations 2 and 3). This approach will be used in the settlement predictions in the following section.

$$C_p = 1.06 * e_0 + 115.61 * (\frac{1}{PFAW}) - 0.45 \text{ , } (R^2=0{,}63) \quad (2A)$$

$$C_p = 12^* \gamma_n^{-4} \text{ , } \quad (R^2=0.56) \quad (2B)$$

$$m_v = 0.0001 * (1.55 * e_0^{\,2} - 2.98 * e_0 + 3.58 * (\frac{1}{PFAW}) + 2.05), \quad (R^2=0{,}71) \quad (3)$$

5 PREDICTION OF THE SETTLEMENT OF FOUNDATIONS

5.1. DIRECT LABORATORY METHOD

A simple oedometer method can be used for settlement predictions at a particular pressure level. The collapse potential may be estimated for an applied stress less than this particular level by calculating the difference in the strain between the inundated and un-inundated curves in an e-log vs P plot, as suggested in ASTM D5333 – 03 [9]. The inundated curve is obtained by drawing a line between the starting point of the dry loading and the end of the collapse. This procedure can be applied in an e-P graph, in which the trend shows polynomial behavior (Figure 9a).

On the test curve the void ratio reductions for loading at the natural water content and collapse (Δe_1 and Δe_2 respectively) corresponding to the incremental pressure (Δp) are determined. The settlement of soil without any change in the natural moisture content (S_1) and the settlement caused by the collapse in the soil structure (S_2) are given by the following expressions:

$$S_1 = \frac{\Delta e_1}{1 + e_o}(H) \quad (4)$$

$$S_2 = \frac{\Delta e_2}{1 + e_1}(H) \quad (5)$$

where H is the thickness of the soil susceptible to collapse, and e_0 , e_1 and e_2 are the void ratios shown in figure 9a.

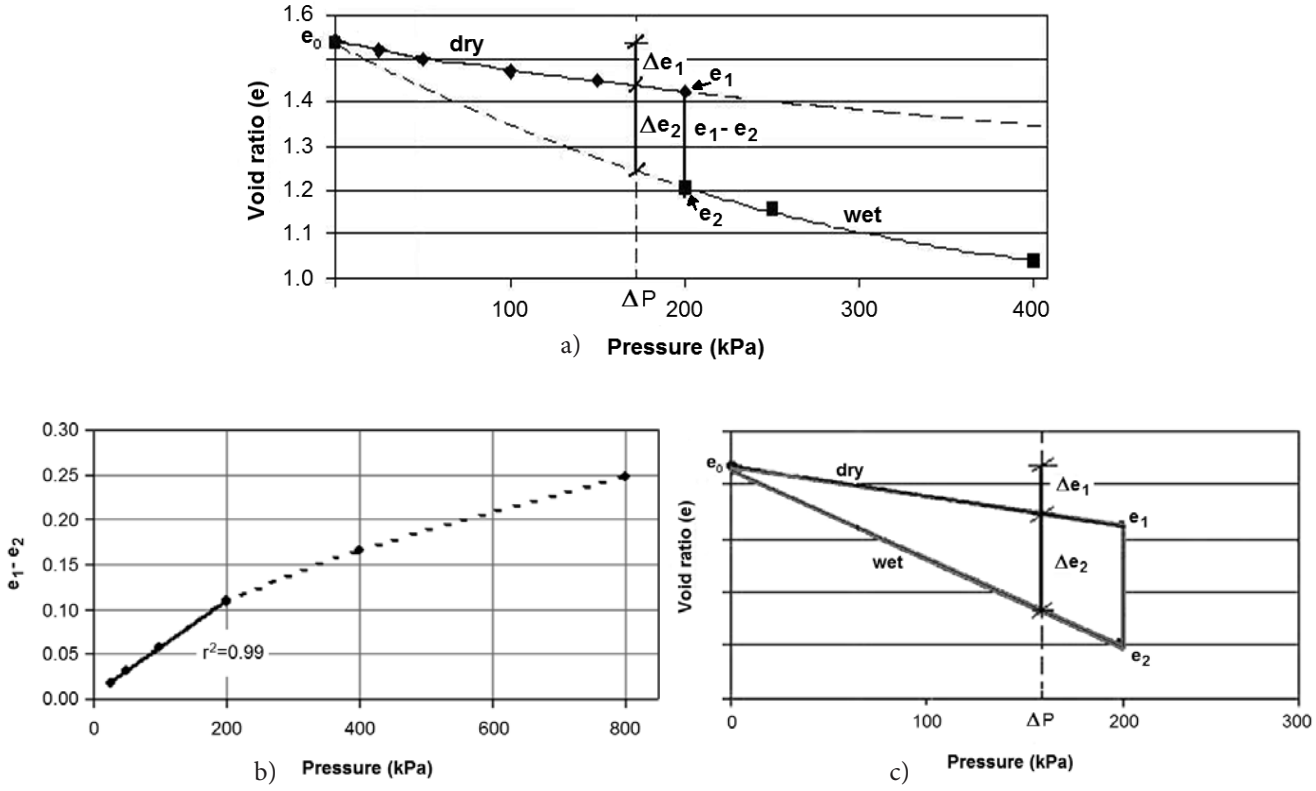

Figure 9. a) Settlement calculation from single oedometer test for a foundation pressures less than 200 kPa (Modified from ASTM 5333), b) For pressures below 200 kPa, Δe_2 changes almost linearly, c) Assumed triangle model used in empirical settlement calculation for foundation pressures less than 200 kPa.

5.2 EMPIRICAL METHOD

Settlements that result from the pore collapse of tufa occur very rapidly. When a stability problem arises, engineers have to make a reliable decision quickly. The technique for determining the collapse potential and to estimate settlement, which is given in the previous sections, is based on undisturbed sampling, careful sample preparation and laboratory testing. However, to have an idea about the soil, the collapse potential calculations and the settlement predictions can be made empirically, in a short time and with less effort. Using the empirical procedure, the collapse potential calculations and the settlement predictions can be made in hours and without the need for complicated laboratory equipment.

The laboratory test results reveal that for small pressures less than 200 kPa, Δe_2 changes almost linearly (Figure 9b). This allows us to assume a triangular shape for the behavior of the collapse for the changing stress levels, as shown in Figure 9c. In this way, Δe_2 for any pressure level less than 200 kPa can be calculated by making a linear interpolation.

The empirical method that is proposed in this study starts with a determination of the dry density. For this purpose, a soil specimen of known volume (V) should be obtained. A sample taken in a steel tube or a cube sample can be used. After determining the mass of the dry soil sample (M), the dry density (ρ_{dry}, Mg/m^3) and the initial void ratio (e_0) can be obtained (G_s = 2.7).

$$\rho_{dry} = \frac{M}{V} \qquad (6)$$

$$e_0 = \frac{G_s}{\rho_{dry}} - 1 \qquad (7)$$

Using a sieve analysis the PFAW can be calculated. Using equations 2 and 3, C_p , (at 200 kPa), m_v (for 100-200 kPa) can be estimated and e_1- e_2 (at 200 kPa), can be calculated.

$$e_1 = e_0 - (m_v.\Delta p.(1+e_0)) \qquad (8)$$

$$e_1 - e_2 = \frac{C_p(1+e_1)}{100} \qquad (9)$$

Using a linear interpolation Δe_2 can be calculated (Equation 10), and using m_v, Δe_1 can be calculated for the pressure level at which the settlement calculations are being carried out (Equation 11).

$$\Delta e_2 = \frac{(e_1 - e_2).(\Delta P)}{200} \qquad (10)$$

$$\Delta e_1 = m_v.\Delta P.(1 + e_0) \qquad (11)$$

The settlement of soil without a change in the moisture content and the settlement caused by any further collapse in the soil structure due to saturation can be calculated using equations 4 and 5, respectively.

To make a comparison between the direct (single ring oedometer) method and the empirical method, the settlement of a 4-m-thick collapsible soil layer is calculated at 100 kPa base pressure making use of the laboratory data from 36 samples. Figure 10 shows the comparison between settlement values calculated with the direct oedometer technique and the empirical method mentioned above. The results of the direct oedometer technique are in close agreement with the empirical method.

6 CONCLUSIONS

(1) The grains in the Antalya tufa deposits are bound together by meniscus cementation, comprising thin calcium carbonate films. Most of the paludal and fluvial environment tufas are made of grain-supported sand and silt size grains. A weak meniscus cementation makes these deposits bonded but with a highly porous soil structure. An increase in the water content can easily dissolve these thin films and destroy the interspatial bonding.

(2) The collapse potential (C_p) values determined from the oedometer tests fall between 0.8% and 14.5%. Most of the studied tufa samples fall into the collapsible class. The collapse potential (C_p) is in a close relation with the initial void ratio (e_0) and the percentage fines after wetting (PFAW). Similarly, a relationship between the coefficient of volume compressibility (m_v), the initial void ratio (e_0) and the percentage fines after wetting (PFAW) was obtained.

(3) The collapsibility of tufas depends on the stress level. The void ratio difference between the dry and wet testing (e_1- e_2) changes almost linearly

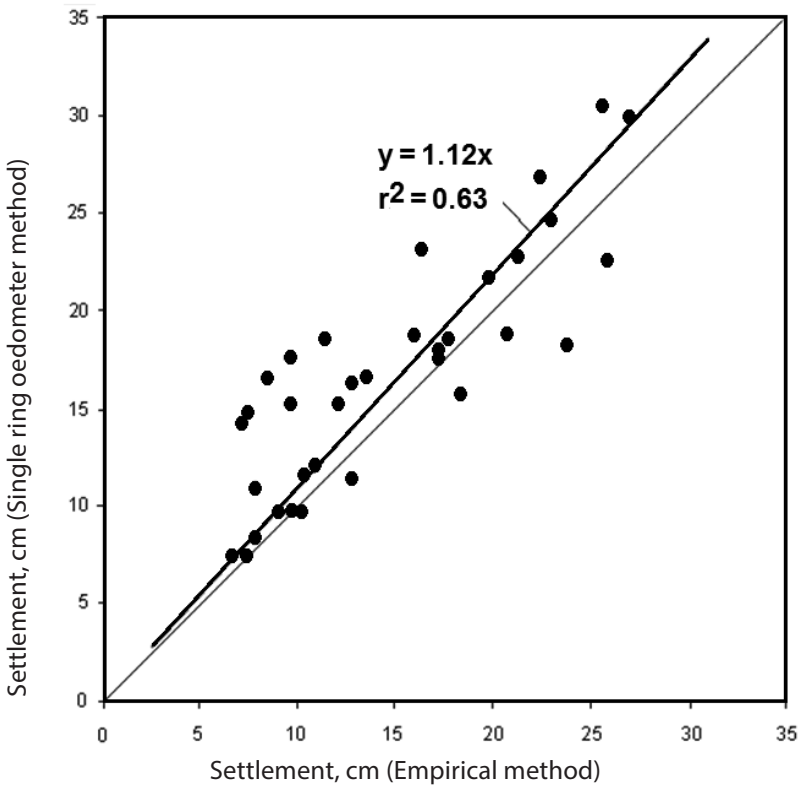

Figure 10. Comparison between settlement calculations using single-ring oedometer and empirical settlement methods.

up to 200 kPa. Thus, for foundation pressures less than 200 kPa, which is common for most low-rise and middle-rise buildings, the collapse potential changes almost linearly with pressure.

(4) The settlement of foundations due to the collapse of a soil structure can be estimated directly and empirically. The direct method is based on undisturbed sampling and an evaluation of the oedometer test results. The indirect method was improved based on the relationship between the collapse potential – index parameters and the coefficient of volume compressibility. The comparison of the direct and empirical approaches yielded good agreement.

ACKNOWLEDGEMENTS

This study was supported by the Research Fund of Akdeniz University (Antalya, Turkey).

REFERENCES

[1] Dipova, N. and Doyuran,V. (2006a). Characterization of the Antalya (Turkey) tufa deposits. Carbonates and Evaporites, 21(2), 144-160.

[2] Dipova, N. and Doyuran, V. (2006b). Assessment of the collapse mechanism of tufa deposits. Engineering Geology, 83, 332-342.

[3] Cuccovillo, T. and Coop, M. R. (1997). Yielding and pre-failure deformation of structured sands. Geotechnique, 47, 3, 491-508.

[4] Leroueil, M. (2000). Contribution to the round table: Peculiar aspects of structured soils. In A. Evangelista and L. Picarelli (Eds.), The geotechnics of hard soils – soft rocks: Proceedings of the second International Symposium on Hard Soils – Soft Rocks, Naples, Italy, 12-14 October 1998 (v.3, pp. 1669-1677). Rotterdam, the Netherlands: A. A. Balkema.

[5 Airey, D. W. (1993). Triaxial testing of naturally cemented carbonate soil. Journal of Geotechnical Engineering, 119,9, 1379-1398.

[6] Denisov, N. Y. (1953). Stroitel'nye Svojstva Loessov I Lessovidnykh Suglinkov (Construction Properties of Loesses and Loessial Soils), Gosstrojizdat, Moscow, CIS.

[7] Dudley, J. G. (1970). Review of collapsing soils. The Journal of Soil Mechanics and Foundation Division ASCE, 96, 925–947.

[8] Reznik, Y. M. (1994). Evaluation of collapse potentials using single oedometer test results. Bulletin of the Association of Engineering Geologists XXXI 2, 255–261

[9] ASTM. (2005). ASTM, D5333-03, Standard test method for measurement of collapse potential of soils, ASTM Standards, Philadelphia, Pennsylvania.

[10] Abelev, Y. M. (1948). The essentials of designing and building on micro-porous soils. Stroital Naya Promyshlemast, No.10.

[11] Derbyshire, E., Meng, X., Wang, J., Zhou, Z. and Li, B. (1995). Collapsible loess on the loess plateau of China. In: E. Derbyshire, T.A. Dijkstra and I.J. Smalley, Ed. Genesis and Properties of Collapsible Soils. NATO ASI Series C: Mathematical and Physical Sciences vol. 468, Kluwer Academic Publishers, Dordrecht, The Netherlands, 267–293.

[12] Jefferson, I. and Smalley, I. (1995). Six definable particle types in engineering soils and their participation in collapse events: proposals and discussions. In E. Derbyshire, T. Dijkstra and I. J. Smalley, ed. Genesis and properties of collapsible soils, NATO ASI Series C: Mathematical and Physical Sciences vol. 468, Kluwer Academic Publishers, Dordrecht, The Netherlands, 19–32.

[13] Lefebvre, G. (1995). Collapse mechanisms and designs for partly saturated soils. In E. Derbyshire, T. Dijkstra and I. J. Smalley, ed. Genesis and properties of collapsible soils, NATO ASI Series C: Mathematical and Physical Sciences vol. 468, Kluwer Academic Publishers, Dordrecht, The Netherlands, 361–374.

[14] Rogers, C. F. D. (1995). Types and distribution of collapsible soils. In E. Derbyshire, T. Dijkstra and I. J. Smalley, ed. Genesis and properties of collapsible soils, NATO ASI Series C: Mathematical and Physical Sciences vol. 468, Kluwer Academic Publishers, Dordrecht, The Netherlands, 1–18.

[15] Torrance, J. K. (1995). Post-depositional processes in high sensitivity, fine grained, collapsible sediments. In E. Derbyshire, T. Dijkstra and I. J. Smalley, ed. Genesis and properties of collapsible soils, NATO ASI Series C: Mathematical and Physical Sciences vol. 468, Kluwer Academic Publishers, Dordrecht, The Netherlands, 295–312.

[16] Rao, S. M. and Revanasiddappa, K. (2002). Collapse behaviour of a residual soil, Geotechnique 52(4), 259–268

[17] Rollins K. M., Rollins R. L., Smith T. D. and Beckwith G. H. (1994). Identification and characterization of collapsible gravels, Journal of geotechnical engineering, 120(3), 528-542.

[18] ASTM. (2000). ASTM D854-00e1, Standard test methods for specific gravity of soil solids by water pycnometer, ASTM Standards, Philadelphia, Pennsylvania.

[19] IAEG. (1981). Rock and soil descriptions for engineering geological mapping. Report by the IAEG

Commission on Engineering Geological Mapping. Bull. Int. Assoc. Eng. Geol. 24, 235–274.
[20] ASTM. (1998). ASTM D422-63, Standard test method for particle-size analysis of soils, ASTM Standards, Philadelphia, Pennsylvania.